

000 APPROXIMATE MULTI-MATRIX MULTIPLICATION FOR 001 STREAMING POWER ITERATION CLUSTERING 002

003 **Anonymous authors**

004 Paper under double-blind review

005 ABSTRACT

006 Given a graph, accurately and efficiently detecting the communities present is
007 one of the main challenges in network analysis. In this era, where datasets rou-
008 tinely exceed terabytes in size, many classical algorithms for solving this prob-
009 lem become computationally prohibitive. We address this challenge in the con-
010 text of the Stochastic Block Model (SBM), which allows for a rigorous analysis.
011 Our approach is a sublinear, updateable, and single-pass approximation to a clas-
012 sic power iteration algorithm (Mukherjee & Zhang, 2024). We introduce two
013 sketching-based variants: (1) a *streaming algorithm* for single-pass processing of
014 edge streams, and (2) an *r-pass algorithm* that achieves a smaller space embedding
015 at the cost of additional passes equal to the power r of the matrix to be approxi-
016 mated. We show that both methods produce vertex embeddings that guarantee the
017 recovery of the largest cluster when performing single-linkage clustering with an
018 appropriate *separation scale* cut threshold.

019 Our key contribution is a new theoretical analysis of Approximate Multi-Matrix
020 Multiplication (AMMM), which guarantees that the error from repeated compres-
021 sion remains manageable. This framework extends the stable-rank-based approxi-
022 mate matrix multiplication (AMM) guarantees of (Cohen et al., 2016) to arbitrarily
023 many conforming matrices. We prove that both algorithms preserve the geometric
024 structure needed to identify the largest community using sublinear space in prac-
025 tice. The streaming algorithm (1) scales with the stable rank of the graph matrix
026 for the streaming algorithm, which we show is sublinear in practice. The r -pass
027 algorithm achieves the optimal $O(\varepsilon^{-2} \log n)$. Experiments on synthetic graphs
028 confirm that our methods can recover the largest community as effectively as the
029 exact, expensive algorithm, across both balanced and unbalanced communities,
030 but with dramatically lower memory and runtime.

031 1 INTRODUCTION

032 Community detection in graphs is a fundamental problem with applications across network anal-
033 ysis, machine learning, and data mining. In this work we focus on spectral methods that learn
034 low-dimensional vertex representations via algebraic measurements of graph matrices. Although
035 these methods remain popular in practice, they face significant scalability challenges in modern
036 datasets, which can be large, evolving, or both. Conventional spectral embedding methods utilize
037 iterative graph decompositions or power iteration stages, requiring access to the whole graph matrix.
038 Furthermore, these embeddings are often difficult to update if the graph evolves, even slightly.

039 In this work we seek to overcome these challenges by designing a turnstile streaming embedding.
040 A turnstile (sometimes called dynamic) streaming algorithm is robust to the addition or deletion of
041 edges, which is essential for evolving or temporal data. Moreover, we seek an embedding that is
042 strongly sublinear in the size of the graph matrix, which is critical when the graph is very large.
043 Our investigation yields a trade-off between pass complexity and embedding size, so in addition to
044 a single-pass streaming algorithm we also analyze an r -pass variant with smaller space.

045 **Our Contribution.** We introduce and analyze two efficient variants of power iteration clustering
046 for the stochastic block model (SBM), both building on the foundation laid by Mukherjee & Zhang
047 (2024). Their work established that power iteration of a centered adjacency matrix $B = A -$

054 $q\mathbf{1}\mathbf{1}^\top$ produces row embeddings where the largest community becomes separable by a *separation*
 055 *scale* threshold. Rather than computing B^r , our algorithms approximate this power iteration using
 056 Johnson-Lindenstrauss transform sketches. Our contributions are:
 057

- 058 • **Streaming Algorithm:** We design a single-pass algorithm for dynamic edge streams
 059 that interleaves randomized sketches between matrix multiplications, computing $\tilde{B}^{(r)} =$
 060 $BS_1^\top S_1 B S_2^\top \dots S_{r-2} B S_{r-1}^\top$ using appropriately sampled Johnson-Lindenstrauss trans-
 061 form matrices S_1, S_2, \dots, S_{r-1} . This enables processing graphs too large for memory
 062 while using sublinear embedding dimensions. Moreover, the sketch factors BS_1^\top and
 063 $S_i B S_{i+1}^\top$ are updatable with both edge insertions and deletions.
- 064 • **r -pass Algorithm:** We also analyze an r -pass variant $B^r S$ that achieves smaller space at
 065 the cost of additional passes a loss of robustness to changes in B .
- 066 • **Theoretical Framework:** We develop *Approximate Multi-Matrix Multiplication*
 067 (AMMM), extending the stable-rank optimal sketching of Cohen et al. (2016) to matrix
 068 chains. For any accuracy parameter $\varepsilon \in (0, 1)$ controlling the relative error in matrix
 069 product approximations, AMMM provides non-trivial guarantees that error accumulates
 070 controllably across additional matrices.
- 071 • **Recovery Guarantees:** We prove both algorithms preserve the separation scale needed
 072 for largest-community recovery, with explicit embedding dimensions: $\tilde{O}(\text{sr}(B)\varepsilon^{-2})$ for
 073 streaming and $O(\varepsilon^{-2} \log n)$ for the stored-matrix setting. It is useful to note that $\text{sr}(B)$
 074 denote the stable rank of B while $\epsilon \in (0, 1)$ is the distortion level introduced by the sketch
 075 matrices used.

076 Our AMMM analysis reveals a crucial *multi-step stability property*: the perturbation from sketching
 077 grows linearly rather than exponentially with iterations. This enables our single-pass streaming ap-
 078 proach, where each sketch can be accumulated independently and combined with a single reduction
 079 thereby making the algorithm practical for distributed and streaming environments.

080 Empirically, we validate that both variants recover the largest community in SBMs while preserv-
 081 ing the theoretical separation scale. We show that this preservation occurs both in the balanced
 082 regime where community sizes are roughly uniform and the unbalanced regimes, where com-
 083 munity sizes are skewed and there are many small communities. The streaming method achieves this
 084 with slightly larger embedding dimensions but requires only one pass, representing a fundamental
 085 trade-off between memory and communication efficiency.

087 2 NOTATIONS, MODEL, AND GOAL

089 In this section, we formalize our compute model and objectives. A graph $G = (V, E)$ is drawn from
 090 an SBM if it comes from the distribution

$$091 G \sim \text{SBM}(n, K, \{s_\ell\}_{\ell=1}^K, p, q), \quad 0 < q < p < 1,$$

092 where n is the number of vertices, K is the number of communities (clusters), and s_ℓ is the size of
 093 community ℓ with $\sum_{\ell=1}^K s_\ell = n$ (we allow unbalanced communities), with p and q defined below.

095 For a positive integer x , define $[x] = \{1, 2, \dots, x\}$. We refer to the vertices by integer indices,
 096 so $V = [n]$. Let $C_\ell \subseteq [n]$ and $|C_\ell| = s_\ell$ denoted the index set and cardinality of community ℓ
 097 respectively. The communities are disjoint, so $V = \bigcup_{\ell=1}^K C_\ell$ and $C_\ell \cap C_{\ell'} = \emptyset$ for all $\ell \neq \ell'$.
 098 We write $s_* = \max_{\ell \in [K]} s_\ell$ and $s_{\min} = \min_{\ell \in [K]} s_\ell$. We correspondingly denote the largest and
 099 smallest communities with C_* and C_{\min} , respectively. For vertices i and j , we use the notation $i \sim j$
 100 when $i, j \in C_\ell$ for some ℓ and $i \not\sim j$ if $i \in C_\ell$ and $j \in C_{\ell'}$, where $\ell \neq \ell'$. So, p and q represent the
 101 probability of an edge connecting i and j when $i \sim j$ and $i \not\sim j$, respectively. The adjacency matrix
 102 $A \in \{0, 1\}^{n \times n}$ is symmetric and, for $i, j \in [n]$,

$$103 A_{ij} \sim \begin{cases} \text{Bernoulli}(p), & \text{if } i \sim j \\ 104 \text{Bernoulli}(q), & \text{if } i \not\sim j. \end{cases}$$

105 Throughout, we write $\|\cdot\|_{\text{op}}$ for the operator norm, which coincides with the spectral norm in
 106 our setting, and $\|\cdot\|_{\text{F}}$ for the Frobenius norm of matrices; the (matrix) stable rank is $\text{sr}(X) :=$
 107 $\|X\|_{\text{F}}^2 / \|X\|_{\text{op}}^2$. We use $\|\cdot\|$ to refer generically to any submultiplicative matrix norm. We write
 108 $\|\cdot\|_2$ for the usual ℓ_2 -norm of vectors.

108 **Centered model.** Following the power–iteration analysis in Mukherjee & Zhang (2024), we work
 109 with the q –centered matrix as defined in their paper:
 110

$$111 \quad B := A - q \mathbf{1} \mathbf{1}^\top = \mathbf{L} + \mathbf{R}, \quad \mathbf{L} := \mathbb{E}[B], \quad \mathbf{R} := B - \mathbf{L}. \quad (1)$$

112 Informally, \mathbf{L} is the *signal* part: a deterministic rank– K block structure that encodes the community
 113 means relative to the baseline level q . Mukherjee & Zhang (2024) show that q can be estimated with
 114 $\frac{d_{\min}}{n}$, where d_{\min} is the smallest degree in G (alternately, the smallest support of a row in A). The
 115 term \mathbf{R} is the *noise* (mean–zero fluctuation) around that signal: it is symmetric and has independent
 116 upper–triangular entries. The centered matrix B is created specifically so the elements of \mathbf{R} have
 117 zero mean and variances $\leq p(1 - q)$. Lemma 2.1 of Mukherjee & Zhang (2024) shows there exists
 118 an absolute constant $C_0 > 0$ such that $\|\mathbf{R}\|_{\text{op}} \leq C_0 \sqrt{p(1 - q)} \sqrt{n}$ with probability at least $1 - n^{-3}$.
 119

120 **Goal: largest–cluster recovery.** Our target is to recover the index set C_* of the largest community.
 121 In the exact algorithm considered in Mukherjee & Zhang (2024), one forms *power features* by taking
 122 rows of B^r (for a modest power r , e.g. $r = O(\log n)$ or a small fixed r) and clusters these row
 123 vectors via single linkage clustering with a separation scale threshold Δ_r . The correctness analysis
 124 in Mukherjee & Zhang (2024) is phrased in terms of a Δ_r : there exist thresholds $\tau_{\text{in}}, \tau_{\text{out}}$ with
 125 margin $\gamma := \tau_{\text{out}} - \tau_{\text{in}} > 0$, such that the within– C_* pairwise row distances of B^r are at most τ_{in}
 126 and the across– C_* vs. $[n] \setminus C_*$ distances are at least τ_{out} .

127 We focus on the setting where A is too large to store and may arrive as a dynamic (turnstile) stream
 128 of edge insertions and deletions. We therefore interleave the powers of B with oblivious sketches
 129 $S_1, \dots, S_r \in \mathbb{R}^{m \times n}$ in the form $\tilde{B}^{(r)} = B S_1^\top S_1 B S_2^\top S_2 \cdots B S_{r-1}^\top S_{r-1} B S_r^\top$. Note that the
 130 linearity of the random projections implies that the individual factors $B S_1^\top$ and $S_i B S_{i+1}^\top$ can be
 131 individually updated with edge insertions and deletions and only multiplied together at clustering
 132 time. Linearity also allows us to apply the $q \mathbf{1} \mathbf{1}^\top$ component of B to the sketches at multiplication
 133 time. Appendix B provides more detail.

134 Our AMMM analysis in §4 and §5 shows that, whenever the power features B^r satisfy the separation
 135 scale Δ_r a *similar* threshold works for \tilde{B}^r , provided the embedding dimension $m = \tilde{O}(\text{sr}(B) \varepsilon^{-2})$
 136 where $\varepsilon \in (0, 1)$ is the distortion introduced by the sketches. We also show a simple analysis in
 137 §5.3 of a simpler r -pass algorithm. We compute $B^r S^\top = B(B(\dots(B S^\top) \dots))$ using a single
 138 sketch $S \in \mathbb{R}^{m \times n}$ in r passes by multiplying the intermediate product by B on the left in each
 139 pass. This is similar to the algorithms considered by Zhang et al. (2018) and Macgregor (2023).
 140 Note that we can apply the rank-one term, $q \mathbf{1} \mathbf{1}^\top$, during each of these multiplications, avoiding
 141 the need to store or multiply using the dense B matrix. A standard Johnson–Lindenstrauss argument
 142 shows multiplicative preservation of all row distances for $m = O(\varepsilon^{-2} \log n)$, so the separation scale
 143 scheme succeeds.

145 3 EXACT POWER ITERATION, ROW DISTANCES, AND THE SEPARATION SCALE

147 We begin by recalling the structure of \mathbf{L} and the separation scale, borrowing from the analysis
 148 in Mukherjee & Zhang (2024). The following is a self-contained derivation.

149 **Lemma 3.1** (Norms of \mathbf{L} and row separation). *We have $\|\mathbf{L}\|_{\text{op}} = (p - q)s_*$ and $\|\mathbf{L}\|_{\text{F}}^2 = (p -$*
 150 $q)^2 \sum_{\ell=1}^K s_\ell^2$. Moreover, rows of \mathbf{L}^r are constant within each cluster and, if $i \in C_\ell$ and $j \in C_{\ell'}$ with
 151 $\ell \neq \ell'$,

$$153 \quad \|L_{i,\cdot}^r - L_{j,\cdot}^r\|_2 = (p - q)^r \sqrt{s_\ell^{2r-1} + s_{\ell'}^{2r-1}}. \quad (2)$$

155 *Proof.* Deferred to Appendix C. □

157 We define the separation scale as

$$158 \quad \Delta_r := (p - q)^r s_*^{r - \frac{1}{2}}. \quad (3)$$

160 Theorem 1.1 of Mukherjee & Zhang (2024) asserts that, if the largest community size s_* and the
 161 separation scale Δ_r are large enough relative to p and q , then the gap between the rows of B^r are
 162 large enough for single linkage clustering to separate the largest cluster.

162 **Theorem 3.1** (Recovering largest cluster (Theorem 1.1 of Mukherjee & Zhang (2024))). *There
163 are constants $C, C_0 > 0$ such that the following holds. Let $p, q \leq 0.75$ be parameters
164 such that $\max\{p(1-p), q(1-q)\} \geq C_0(\log n)/n$. Let G be a random graph sampled from
165 SBM($n, K, \{s_\ell\}_{\ell=1}^K, p, q$), and let s_* be the size of the largest cluster.¹ If $s_* \geq C \cdot (\log n)^7 \cdot$
166 $\sqrt{p(1-q)} \cdot \sqrt{n}/(p-q)$, then with probability $1 - O(1/n)$ one of the clusters produced by Al-
167 gorithm 1 is the largest cluster of G for $\Delta_r = \frac{1}{2}\sqrt{s^*}(p-q)^r(s^*)^{r-1}$ and $r = \lceil \log n \rceil$.*
168

169 Our proofs use the following assumption that naturally follows given the conditions of Theorem 3.1.
170

171 **Assumption 3.2** (Unsketched separation scale). *There exist $0 < a < b, \eta > 0$ very small and power
172 r such that with probability at least $1 - \eta$ over the graph,*

$$173 \quad i \sim j \Rightarrow \|B_{i,\cdot}^r - B_{j,\cdot}^r\|_2 \leq a \Delta_r, \quad i \not\sim j \Rightarrow \|B_{i,\cdot}^r - B_{j,\cdot}^r\|_2 \geq b \Delta_r.$$

175 We are now able present our algorithmic framework. Algorithm 1 represents our chassis for
176 all algorithms considered, as they vary only in the implementation of the embedding subroutine
177 PI_SUBROUTINE. Algorithm 1.1 in Mukherjee & Zhang (2024) corresponds to the clustering Al-
178 gorithm 1 using Subroutine A as PI_SUBROUTINE. We will abuse notation and refer to this com-
179 position as Algorithm A for brevity, and similarly to the streaming and r -pass variants as Algorithm B
180 and Algorithm C, respectively. Appendix B explains the streaming update behavior of Subroutine B
181 in more explicit terms. The correctness of Algorithm A is guaranteed by Theorem 3.1 (Theorem 1.1
182 of Mukherjee & Zhang (2024)), while we will show the correctness of Algorithms B and C.
183

184 **Algorithm 1** DETECTING COMMUNITIES BY POWER ITERATION FRAMEWORK

185 1: **Input:** A graph G and parameters $p, q > 0$.
186 2: Let A be the adjacent matrix of G
187 3: $B \leftarrow A - q\mathbf{1}\mathbf{1}^\top$ # (Here $\mathbf{1}^{n \times n}$ is the all 1 matrix.)
188 4: Let $\Delta_r > 0$ and $r > 1$ be parameters # (We will explain how to choose them later)
189 5: $R^{(r)} \leftarrow \text{PI_SUBROUTINE}(B, r)$
190 6: **for** $v_i, v_j \in G$ **do**
191 7: **if** $\|R_i^{(r)} - R_j^{(r)}\|_2 \leq \Delta_r$ **then** # ($R_i^{(r)}$ represents the i -th row of $R^{(r)}$)
192 8: Put v_i and v_j in a same cluster
193 9: **end if**
194 10: **end for**
195 11: Output the sets thus formed.

198 Subroutine A Exact PI	199 Subroutine B Streaming PI	200 Subroutine C r -pass PI
1: Input: $B, r > 1$	1: Input: $B, r > 1$	1: Input: $B, r > 1$
2: Output B^r	2: Sample $S_1, \dots, S_{r-1} \in \mathbb{R}^{m \times n}$	2: Sample $S \in \mathbb{R}^{m \times n}$
	3: Output $BS_1^\top \prod_{i=1}^{r-1} S_i B S_{i+1}^\top$	3: Output $B^r S^\top$

203 Armed thus with the prior work of Mukherjee & Zhang (2024), we are ready to proceed to prove
204 largest cluster guarantees for Algorithm B.
205

206 4 APPROXIMATE MULTI-MATRIX MULTIPLICATION (AMMM)

208 This section extends *approximate matrix multiplication* (AMM) from a pair of products to *com-
209 positions of linear operators* with sketches inserted between consecutive factors. This framework
210 arises naturally in iterative methods like power iteration, where we aim to replace exact matrix pow-
211 ers with sketched approximations while preserving downstream geometric guarantees. Our results
212 hold for any *submultiplicative* matrix norm $\|\cdot\|$ (e.g., spectral or Frobenius) with AMM guarantees.
213 Proof details appear in the appendix; here we provide a self-contained summary sufficient for later
214 applications.
215

¹Our parameterization of SBM differs from Mukherjee & Zhang (2024), who ignore the cluster sizes.

216 4.1 SETUP AND ONE-STEP AMM
217218 Let $A_1, \dots, A_k \in \mathbb{R}^{n \times n}$ be matrices and $S_1, \dots, S_{k-1} \in \mathbb{R}^{m \times n}$ be independent sketching matrices.
219 We compare the exact product $M_k := A_1 A_2 \cdots A_k$ with its sketched counterpart:

220
$$\widetilde{M}_k := A_1 S_1^\top S_1 A_2 S_2^\top S_2 \cdots A_{k-1} S_{k-1}^\top S_{k-1} A_k. \quad (4)$$

221

222 **Definition 4.1** (One-Step (ε, δ) AMM). A matrix $S \in \mathbb{R}^{m \times n}$ satisfies one-step AMM at accuracy
223 (ε, δ) for a norm $\|\cdot\|$ if for all conformable X, Y :

224
$$\Pr \left[\|XS^\top SY - XY\| \leq \varepsilon \|X\| \|Y\| \right] \geq 1 - \delta. \quad (5)$$

225

227 Oblivious sketches satisfying equation 5 are well-studied. In particular, the stable-rank-optimal
228 results of Cohen et al. (2016) achieve equation 5 when factors have bounded stable rank. We deliber-
229 ately keep the sketch dimension m implicit until applying AMMM to clustering.230 4.2 MAIN BOUND AND PROOF SKETCH
231232 **Theorem 4.2** (AMMM from One-Step AMM). Assume equation 5 holds for independent
233 S_1, \dots, S_{k-1} . Then with probability at least $1 - ck\delta$ for an absolute constant c :

234
$$\|\widetilde{M}_k - M_k\| \leq \sum_{t=1}^{k-1} \varepsilon (1 + \varepsilon)^{k-1-t} \|A_1 \cdots A_t\| \|A_{t+1} \cdots A_k\|. \quad (6)$$

235

236 In particular, by submultiplicativity:

237
$$\|\widetilde{M}_k - M_k\| \leq ((1 + \varepsilon)^{k-1} - 1) \prod_{i=1}^k \|A_i\|. \quad (7)$$

238

239 *Proof.* Define $M_t := A_1 \cdots A_t$ and $\widetilde{M}_t := A_1 S_1^\top S_1 \cdots A_{t-1} S_{t-1}^\top S_{t-1} A_t$. The proof proceeds by:240 1. Adding and subtracting $M_t S_t^\top S_t A_{t+1}$ at each step
241 2. Applying the one-step guarantee equation 5 twice (once for M_t , once for the error $\widetilde{M}_t - M_t$)
242 3. Obtaining the recurrence:

243
$$\|\widetilde{M}_{t+1} - M_{t+1}\| \leq \varepsilon (\|M_t\| + \|\widetilde{M}_t - M_t\|) \|A_{t+1}\|.$$

244

245 4. Recursively expanding this recurrence yields equation 6
246 5. Applying submultiplicativity $\|M_t\| \leq \prod_{i=1}^t \|A_i\|$ gives equation 7247 The probability bound follows from applying the one-step result $O(k)$ times with a union bound. \square
248249 Theorem 4.2 establishes an upper bound for AMMM, but at this time a corresponding lower bound
250 for general k is an open problem. Notably for $k = 2$, Theorem 4.2's upper bound corresponds to the
251 tight lower bound Cohen et al. (2016).252 **Corollary 4.3** (Power Chains). If $A_1 = \cdots = A_k = B$, then with the same probability as The-
253 rem 4.2:

254
$$\|BS_1^\top S_1 B S_2^\top S_2 \cdots B S_{k-1}^\top S_{k-1} B - B^k\| \leq ((1 + \varepsilon)^{k-1} - 1) \|B\|^k. \quad (8)$$

255

256 *Proof.* Direct application of Theorem 4.2 with all $A_i = B$. \square
257258 The inequality equation 6 shows that *local* one-step AMM errors accumulate controllably rather
259 than exploding across the chain. This enables replacing iterative multiplications (with dimension n)
260 with streaming sketch accumulation followed by the multiplication of several small sketch matrices
261 (where most products have dimension $m \ll n$). Moreover, the sketch components of AMMM can

270 be accumulated from a turnstile stream. Corollary 4.3 ensures accuracy preservation for downstream
 271 tasks like clustering.

272 To use AMMM in practice, instantiate the one-step hypothesis equation 5. For example, Cohen et al.
 273 (2016) show that for sketches with dimension determined by the stable rank of factors, equation 5
 274 holds. Plugging such an AMM into Theorem 4.2 yields AMMM for the interleaved form equation 4.
 275 We explore sketch dimension choices for clustering in §5, where the pass-memory tradeoff becomes
 276 meaningful.

278 5 FROM STABLE RANK AMM TO STREAMING CLUSTERING

280 We combine the stable rank dependent approximate matrix multiplication result of Cohen et al.
 281 (2016) with the AMMM bounds from §4 to obtain explicit, sublinear embedding dimensions that
 282 preserve the row distance threshold in Assumption 3.2. Throughout, set $X^* := B^r$.

284 5.1 STABLE RANK AMM

286 We use a subgaussian sketch bound that depends only on the operator norm and the stable rank. We
 287 begin by recalling the Oblivious Subspace Embedding (OSE) moment property.

288 **Definition 5.1** (OSE moment property). *A distribution \mathcal{D} over $\mathbb{R}^{m \times n}$ has the $(\varepsilon, \delta, s, \ell)$ OSE moment
 289 property if for every matrix $U \in \mathbb{R}^{n \times d}$ with orthogonal columns,*

$$290 \mathbb{E}_{\Pi \sim \mathcal{D}} \|(\Pi U)^T (\Pi U) - I\|^\ell < \varepsilon^\ell \delta.$$

292 We now state the main lemma from Cohen et al. (2016), which will be used to obtain our embedding
 293 dimensions.

294 **Theorem 5.2** (Theorem 1 of Cohen et al. (2016)). *Let $k \geq 1$ and $\varepsilon, \delta \in (0, 1/2)$. Suppose $\Pi \in$
 295 $\mathbb{R}^{m \times n}$ is drawn from a distribution that satisfies the $(\varepsilon, \delta, 2k, \ell)$ OSE moment property for some
 296 $\ell \geq 2$. Then for any A, B ,*

$$297 \Pr \left\{ \|(\Pi A)^T (\Pi B) - A^T B\|_{op} \leq \varepsilon \sqrt{\left(\|A\|_{op}^2 + \frac{\|A\|_F^2}{k} \right) \left(\|B\|_{op}^2 + \frac{\|B\|_F^2}{k} \right)} \right\} \geq 1 - \delta. \quad (9)$$

300 Moreover, for a Rademacher or subgaussian sketch,

$$302 m \geq C \frac{k + \log(1/\delta)}{\varepsilon^2} \implies \Pi \text{ satisfies the } (\varepsilon, \delta, 2k, \Theta(k + \log(1/\delta))) \text{ OSE moment property,} \quad (10)$$

304 which implies equation 9. If $k \geq \max\{\text{sr}(A), \text{sr}(B)\}$, the bound simplifies to

$$306 \|(\Pi A)^T (\Pi B) - A^T B\|_{op} \leq 2\varepsilon \|A\|_{op} \|B\|_{op}. \quad (11)$$

307 We next derive a high probability bound on the stable rank of the shifted adjacency matrix B .

309 **Lemma 5.1** (High probability upper bound on $\text{sr}(B)$). *Let $G \sim \text{SBM}(n, K, \{s_\ell\}, p, q)$ with adja-
 310 cency matrix A . Let B, L , and R be defined as in equation 1. Write $s_* = \max_\ell s_\ell$ and define*

$$311 \sigma^2 = \max\{p(1-p), q(1-q)\}.$$

312 There exist constants $C_1, C_2 > 0$ such that, with probability at least $1 - 3n^{-3}$,

$$314 \text{sr}(B) = \frac{\|B\|_F^2}{\|B\|_{op}^2} \leq \frac{(p-q)^2 \sum_{\ell=1}^K s_\ell^2 + n^2 \sigma^2 + C_1 n \sqrt{\log n}}{((p-q)s_* - C_2 \sigma \sqrt{n})^2}. \quad (12)$$

316 In particular, under the signal-dominated regime $(p-q)s_* \gg \sigma\sqrt{n}$:

318 • **Balanced case** ($s_\ell = n/K$):

$$320 \text{sr}(B) = O \left(K + \frac{K^2 \sigma^2}{(p-q)^2} \right).$$

322 If additionally $(p-q)^2 \gtrsim K\sigma^2$, then $\text{sr}(B) = \Theta(K)$. More generally, under the weaker
 323 detectability condition $(p-q)^2 \gtrsim K^2\sigma^2/n$ (which follows from $(p-q)s_* \gg \sigma\sqrt{n}$ with
 $s_* = n/K$), we have $\text{sr}(B) = o(n)$, confirming sublinearity.

- *Highly imbalanced case* ($\sum_\ell s_\ell^2 \asymp s_*^2$):

$$\text{sr}(B) = O\left(1 + \frac{n^2\sigma^2}{(p-q)^2s_*^2}\right).$$

If $(p - q)s_* \gg \sigma n$, then $\text{sr}(B) = \Theta(1)$.

Proof. Deferred to Appendix C.

The next lemma converts an operator norm bound on a product approximation into a bound on all pairwise row distances. This lets us transfer a global AMMM error bound into a guarantee for the separation scale.

Lemma 5.2 (Product implies row distances). *For $M, \widetilde{M} \in \mathbb{R}^{n \times d}$ with $E = \|\widetilde{M} - M\|_{op}$, for all $i \neq j$,*

$$\left| \|\widetilde{M}_{i,\cdot} - \widetilde{M}_{j,\cdot}\|_2 - \|M_{i,\cdot} - M_{j,\cdot}\|_2 \right| \leq \sqrt{2} E. \quad (13)$$

Proof. Let $u = e_i - e_j$. Then

$$\|u^T \widetilde{M}\|_2 - \|u^T M\|_2 \leq \|u^T(\widetilde{M} - M)\|_2 \leq \|u\|_2 E = \sqrt{2}E.$$

5.2 MAIN STREAMING THEOREM (EXPLICIT SUBLINEAR m)

We now state the main streaming result with an explicit embedding dimension.

Theorem 5.3 (Separation scale preservation for streaming Algorithm B; explicit m). *Assume Assumption 3.2 holds for $X^* = B^r$ with parameters (a, b, Δ_r) and failure probability η . Fix $\varepsilon \in (0, 1/4)$ and $\delta \in (0, 1)$. Suppose $S_1, \dots, S_{r-1} \in \mathbb{R}^{m \times n}$ are independent Rademacher matrices with*

$$m \geq C \frac{\text{sr}(B) + \log((r-1)/\delta)}{\varepsilon^2}. \quad (14)$$

Then, with probability at least $1 - \eta - 2\delta$, for all $i \neq j$,

$$\left| \|\widetilde{B}_{i,\cdot}^{(r)} - \widetilde{B}_{j,\cdot}^{(r)}\|_2 - \|B_{i,\cdot}^r - B_{j,\cdot}^r\|_2 \right| \leq \sqrt{2} \left((1+2\varepsilon)^{r-1} - 1 \right) \|B\|_{op}^r. \quad (15)$$

If, in addition, there exist $0 < a < b$ such that

$$\sqrt{2}((1+2\varepsilon)^{r-1}-1)\|B\|_{op}^r \leq \frac{b-a}{4}\Delta_r, \quad (16)$$

then the threshold Δ_r still separates within-cluster and across-cluster pairs for $\widetilde{B}^{(r)}$, and single linkage at cut Δ_r recovers the largest cluster.

Proof. Deferred to Appendix C.

Note that Theorem 4.2 states the bound on embedding dimension m in terms of dense Rademacher $\{\pm 1\}$ matrices. A similar argument yields a slightly larger bound for sparse Johnson-Lindenstrauss transforms, such as those implemented with CountSketch Cohen et al. (2016). While such transforms will yield better runtime performance in practice, we have omitted it for space.

5.3 r -PASS VARIANT WITH EXPLICIT m

We now present a similar separation guarantee for Algorithm C. This variant is practical when A is static and its edge stream can be warehoused and read in multiple passes, and the cost of each sparse product of the form AS^T is low. In this setting, sketching B^rS^T leads to a lower effective bound on m at the cost of requiring r passes over A .

378 **Theorem 5.4** (Separation scale preservation for r -pass Algorithm C; explicit m). *Let $X^* = B^r \in \mathbb{R}^{n \times n}$ with rows x_i^* . Assume Assumption 3.2 holds for X^* with parameters (a, b, Δ_r) and success probability $1 - \eta$. In other words, with probability at least $1 - \eta$,*

$$382 \quad \|x_i^* - x_j^*\|_2 \leq a \Delta_r \quad (\text{within}), \quad \|x_i^* - x_j^*\|_2 \geq b \Delta_r \quad (\text{across}).$$

383 Let $S \in \mathbb{R}^{m \times n}$ have independent mean-zero variance- $1/m$ subgaussian entries with subgaussian 384 norm at most κ . Fix $\varepsilon \in (0, 1)$ and $\delta \in (0, 1)$. If

$$386 \quad m \geq \frac{C(\kappa)}{\varepsilon^2} (\log n + \log(1/\delta)), \quad (17)$$

388 then with probability at least $1 - \eta - \delta$, for all $i \neq j$,

$$389 \quad (1 - \varepsilon) \|x_i^* - x_j^*\|_2 \leq \|S(x_i^* - x_j^*)\|_2 \leq (1 + \varepsilon) \|x_i^* - x_j^*\|_2.$$

390 If, in addition,

$$392 \quad (1 + \varepsilon)a < (1 - \varepsilon)b, \quad (18)$$

393 then there exists a threshold

$$394 \quad \tilde{\Delta} \in ((1 + \varepsilon)a \Delta_r, (1 - \varepsilon)b \Delta_r)$$

395 that separates within-cluster and across-cluster pairs for the sketched rows $\{Sx_i^*\}$, and Algorithm C 396 recovers the largest cluster.

397 *Proof.* Deferred to Appendix C. \square

400 **Takeaway.** The explicit bounds equation 14, equation 17 coupled with the fact that $\text{sr}(B) \leq 401 \text{rank}(B) = o(n)$ show that the embeddings are sublinear: $m = \tilde{O}(\text{sr}(B)/\varepsilon^2)$ for the streaming 402 scheme and $m = O(\varepsilon^{-2} \log n)$ for the r -pass scheme. Both preserve the decision threshold Δ_r 403 used by the unsketched method.

405 6 EXPERIMENTAL EVALUATION

408 We empirically validate that (i) the streaming and r -pass variants preserve the separation scale from 409 Assumption 3.2, (ii) the required embedding dimension m is *sublinear* (scales with $\text{sr}(B)$ or $\log n$), 410 and (iii) the resulting clustering recovers the largest community efficiently.

412 6.1 METHODOLOGY

413 **Synthetic data generation.** We generate graphs from $\text{SBM}(n, K, \{s_\ell\}, p, q)$ as in §2, considering 414 the following parameters. Our SBM generator does not sample self loops, although our theory 415 allows for them. We fix $n = 10^4$ and choose $K \in \{5, 10, 20\}$. We vary $s_*/s_{\min} \in \{1, 2, 4, 8\}$. 416 In our SBM generator, we set an imbalance parameter $\text{imbalance} \in [0, 1]$ interpolating community 417 sizes: $\text{imbalance} = 0$ gives equal sizes, while $\text{imbalance} = 1$ yields a largest community of 418 size s^* and others of size at least $(q/p)s^*$. Choose $p = q + C_1$ where $C_1 > 0.1$ to sweep the 419 operator $\text{SNR} \frac{(p-q)s^*}{\sqrt{p(1-q)}\sqrt{n}}$ from below to above the recovery threshold. We consider the matrix 420 power $r \in \{2, 3, 4\}$. For each setting we run 5 independent trials with different random seeds and 421 report the average of the evaluation metrics.

423 **Methods compared.** We implemented Algorithms B and C with independent Rademacher 424 sketches. We size m for both using the *theory line* from Theorem 5.3 and Theorem 5.4, respectively.

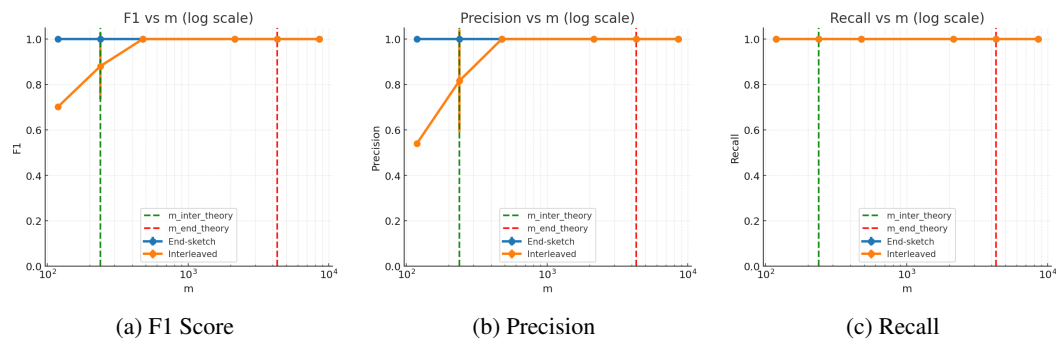
$$427 \quad m_{\text{inter}} = C \frac{\widehat{\text{sr}}(B) + \log((r-1)/\delta)}{\varepsilon^2}, \quad m_{\text{end}} = \frac{8}{\varepsilon^2} \left(\log \binom{n}{2} + \log(2/\delta) \right).$$

429 where C is some constant and $\widehat{\text{sr}}(B) = \|B\|_{\text{F}}^2 / \|\widehat{B}\|_{\text{op}}^2$ with $\|\widehat{B}\|_{\text{op}}$ estimated by power iteration (10 430 steps sufficed in all runs). We also sweep $m \in \{0.5, 1, 2\} \cdot m_*$ for $m_* \in \{m_{\text{inter}}, m_{\text{end}}\}$. In all 431 experiments we fixed $\varepsilon \in \{0.1, 0.2, 0.3\}$ and $\delta = 0.05$ unless otherwise noted.

432 **Metrics.** We collect the largest cluster output by our algorithms as \widehat{C}_* and compare it with the true
 433 largest community C_* . We report (i) *Largest-cluster recall* $\text{Rec}_* = \frac{|\widehat{C}_* \cap C_*|}{|C_*|}$; (ii) *Largest-cluster*
 434 precision $\text{Prec}_* = \frac{|\widehat{C}_* \cap C_*|}{|\widehat{C}_*|}$; (iii) *Largest-cluster F1*, $\text{F1}_* = 2 \frac{\text{Rec}_* \text{Prec}_*}{\text{Rec}_* + \text{Prec}_*}$; (iv) and *Row-gap margin*
 435 $M = \min_{i \neq j} \text{dist}(i, j) - \max_{i \sim j} \text{dist}(i, j)$ at the chosen $\widehat{\Delta}$.
 436
 437

438 6.2 RESULTS

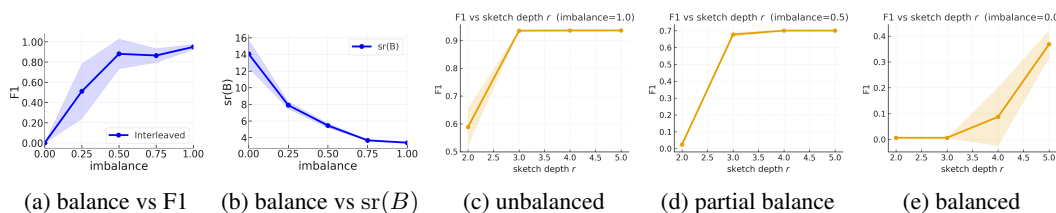
440 **Largest cluster recovery.** Figure 1 plots largest-cluster recall, precision, and F1 for fixed
 441 (n, K, p, q, r) as we sweep m for both Algorithms B and C. Figure 1c shows dimension normaliza-
 442 tion across n and verifies that recall saturates near 1 once $m \gtrsim c \widehat{s}(B)/\varepsilon^2$. End-sketch acts as a
 443 comparator with $m = O(\varepsilon^{-2} \log n)$.
 444



456 Figure 1: Parameters: $n = 10^4, K = 5, \text{imbalance} = 0.5, p = 0.3, q = 0.01$
 457

458 Figure 1 shows that the r -pass pipeline always perfectly recovers the largest cluster as long as the
 459 embedding dimension bound is satisfied. Moreover, it shows that the performance of the stream-
 460 ing approach improves drastically as the embedding dimension increases. This confirms the noise
 461 introduced by interleaved sketches is inversely proportional to the embedding dimension.
 462

463 **The effects of imbalance and power.** Figure 2 shows the effects of varying the imbalance, which
 464 is directly proportional to s_*/s_{\min} , and how it interacts with the matrix power r . We observe that as
 465 the imbalance increases, the largest community grows, so the threshold $\Delta = \frac{1}{2}(p-q)^r(s^*)^{r-\frac{1}{2}}$ rises
 466 and points from that community become relatively closer to one another than to the rest; this makes
 467 them easier to separate, so the $F1$ score improves. At the same time the graph is dominated by
 468 that one community, so the matrix B is effectively simpler and its stable rank drops (most variation
 469 now comes from one direction). Consequently, higher imbalance yields both better clustering and a
 470 smaller sketch size when we choose $m \propto \text{sr}(B)$. We sweep $r \in \{2, 3, 4\}$. Larger r increases separation
 471 scale Δ_r (Lemma 3.1) but also increases sensitivity to operator norm growth in the AMMM
 472 bound. We show recall and margin M vs. r . The value of m is dictated by the formula m_{inter} .
 473



480 Figure 2: 2a and 2b show the relationship between imbalance and F1 and $\text{sr}(B)$, respectively. 2c,
 481 2d, and 2e show how F1 improves with r for balanced vs. unbalanced graphs.
 482

483 **Separation scale preservation.** Figure 3 demonstrates that given a reasonable embedding dimen-
 484 sion the same threshold we used for clustering the graph still applied to both Algorithms B and C.
 485 This allows us to visualize Theorem 5.3 and 5.4 at the level of the separation scale.
 486

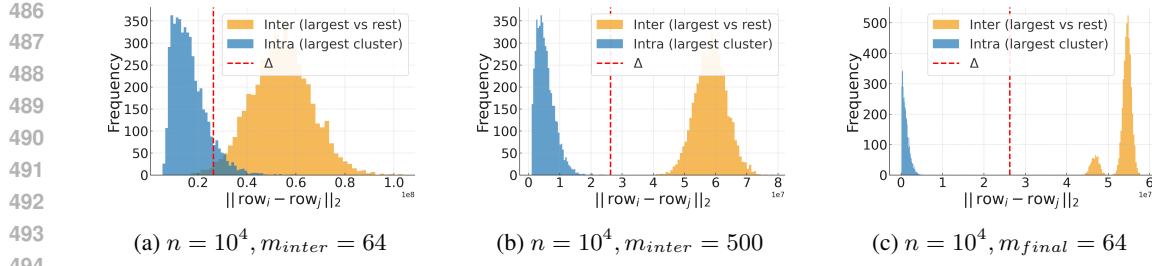


Figure 3: Row distance histograms for different embedding dimensions and embedding approaches.

Across all experiments, the intra-cluster distances in the largest cluster concentrate well to the left of the fixed separation scale Δ_r , while the inter-cluster distances lie to the right when the sketch is sufficiently large, giving clear separation. When we shrink the dimension to 64, the r -pass variant still shows a clean gap, but the streaming algorithm develops visible overlap around Δ , indicating that too small an m injects enough noise to blur the boundary. Thus, in this setting the Δ_r separation scale is preserved for both methods, although the streaming case requires larger m , as suggested by theory.

7 CONCLUSION

We have analyzed and demonstrated a novel turnstile streaming power iteration clustering algorithm utilizing approximate multi-matrix multiplication and oblivious subspace embeddings. Our experiments directly demonstrate a practical sublinear embedding dimension for largest cluster recovery, validating Theorems 5.3 and 5.4. Obvious future work includes an analysis of the recovery of all clusters, as well as an examination of the removal of the awkward centering step required in Algorithm 1. It would also be desirable to find a space lower bound for the approximate multi matrix multiplication problem. Furthermore, although our experiments are relatively unoptimized and sequential, Algorithms B and C are easy to implement in a distributed computing model and will be interesting to demonstrate on billion-scale data.

8 ACKNOWLEDGEMENTS

This work was performed under the auspices of the U.S. Department of Energy by Lawrence Livermore National Laboratory under Contract DE-AC52-07NA27344 (LLNL-CONF-2011640), and was supported by LLNL LDRD project 24-ERD-024.

REFERENCES

- Dimitris Achlioptas. Database-friendly random projections: Johnson-lindenstrauss with binary coins. *Journal of computer and System Sciences*, 66(4):671–687, 2003.
- Christos Boutsidis, Prabhanjan Kambadur, and Alex Gittens. Spectral clustering via the power method-provably. In *International conference on machine learning*, pp. 40–48. PMLR, 2015.
- Moses Charikar, Kevin Chen, and Martin Farach-Colton. Finding frequent items in data streams. In *International Colloquium on Automata, Languages, and Programming*, pp. 693–703. Springer, 2002.
- Haochen Chen, Syed Fahad Sultan, Yingtao Tian, Muhaao Chen, and Steven Skiena. Fast and accurate network embeddings via very sparse random projection. In *Proceedings of the 28th ACM international conference on information and knowledge management*, pp. 399–408, 2019.
- Kenneth L Clarkson and David P Woodruff. Low-rank approximation and regression in input sparsity time. *Journal of the ACM (JACM)*, 63(6):1–45, 2017.
- Michael B. Cohen, Jelani Nelson, and David P. Woodruff. Optimal approximate matrix product in terms of stable rank, 2016. URL <https://arxiv.org/abs/1507.02268>.

540 Nathan Halko, Per-Gunnar Martinsson, and Joel A Tropp. Finding structure with randomness:
 541 Probabilistic algorithms for constructing approximate matrix decompositions. *SIAM review*, 53
 542 (2):217–288, 2011.

543

544 William B Johnson, Joram Lindenstrauss, et al. Extensions of lipschitz mappings into a hilbert
 545 space. *Contemporary mathematics*, 26(189-206):1, 1984.

546

547 Daniel M Kane and Jelani Nelson. Sparser johnson-lindenstrauss transforms. *Journal of the ACM*
 548 (*JACM*), 61(1):1–23, 2014.

549

550 Ping Li, Trevor J Hastie, and Kenneth W Church. Very sparse random projections. In *Proceedings*
 551 *of the 12th ACM SIGKDD international conference on Knowledge discovery and data mining*,
 552 pp. 287–296, 2006.

553

554 Frank Lin and William W Cohen. Power iteration clustering. In *Proceedings of the 27th Interna-*
 555 *tional Conference on International Conference on Machine Learning*, pp. 655–662, 2010.

556

557 Peter Macgregor. Fast and simple spectral clustering in theory and practice. *Advances in Neural*
 558 *Information Processing Systems*, 36:34410–34425, 2023.

559

560 Chandra Sekhar Mukherjee and Jiapeng Zhang. Detecting hidden communities by power iterations
 561 with connections to vanilla spectral algorithms. In *Proceedings of the 2024 Annual ACM-SIAM*
 562 *Symposium on Discrete Algorithms (SODA)*, pp. 846–879. SIAM, 2024.

563

564 Jelani Nelson and Huy L Nguyễn. Sparsity lower bounds for dimensionality reducing maps. In
 565 *Proceedings of the forty-fifth annual ACM symposium on Theory of computing*, pp. 101–110,
 566 2013.

567

568 David P Woodruff et al. Sketching as a tool for numerical linear algebra. *Foundations and Trends®*
 569 *in Theoretical Computer Science*, 10(1–2):1–157, 2014.

570

571 Ziwei Zhang, Peng Cui, Haoyang Li, Xiao Wang, and Wenwu Zhu. Billion-scale network embed-
 572 ding with iterative random projection. In *2018 IEEE international conference on data mining*
 573 (*ICDM*), pp. 787–796. IEEE, 2018.

574

575

576 A RELATED WORK

577

578 For a symmetric, square graph matrix M , power iteration amounts to estimating the eigenvectors by
 579 repeated multiplication by a oblivious subspace embedding matrix S so that the columns of $M^r S$
 580 for some small r can stand in for M ’s top eigenvectors. Many investigators have analyzed orthonor-
 581 malizing and/or decomposing $M^r S$ to prove approximation guarantees to the eigenvectors (Halko
 582 et al., 2011; Woodruff et al., 2014), while others focus on various guarantees in the context of k-
 583 means clustering (Boutsidis et al., 2015; Macgregor, 2023; Lin & Cohen, 2010). While the majority
 584 of these analyses require dense i.i.d. Guassian transforms S , realizing and applying such a matrix
 585 is impractical for very large graphs. Fortunately, dense Gaussian matrices are but one distribu-
 586 tion satisfying the conditions of the famous Johnson-Lindenstrauss lemma (Johnson et al., 1984).
 587 Achlioptas (2003) introduced scaled dense $\{+1, -1\}$ matrices of zero-mean Rademacher variables,
 588 while several works introduced sparsity and eventually worked out tight sparsity bounds (Li et al.,
 589 2006; Nelson & Nguyễn, 2013; Kane & Nelson, 2014). In parallel, Clarkson & Woodruff (2017)
 590 introduced a maximally sparse matrix distribution based upon the famous Count-Sketch data struc-
 591 ture (Charikar et al., 2002), which can be shown to satisfy the same sparsity bounds Cohen et al.
 592 (2016). Some investigators have focused on empirically demonstrating the performance of power
 593 iteration utilizing these more practical sparse Johnson-Lindenstrauss transforms (Zhang et al., 2018)
 or polynomials thereof (Chen et al., 2019), although these analyses are lacking analytic guarantees
 for clustering or other downstream tasks.

594 **B STREAMING UPDATES**
595

596 Here we make the streaming nature of Subroutine B more explicit. The approximate power iteration
 597 subroutine's goal is to output the product $\tilde{B}^{(r)} \equiv BS_1^\top \prod_{i=1}^{r-1} S_i BS_{i+1}^\top$. First, we recall that $B \leftarrow$
 598 $A - q\mathbf{1}\mathbf{1}^\top$. As the $q\mathbf{1}\mathbf{1}^\top$ component is constant and all operations are linear, we can safely defer
 599 its incorporation to the sketches to the end and primarily reason about A . Here Subroutine D shows
 600 how Subroutine B handles a stream σ of updates of the form (i, j, w) to A . Let \hat{A} be a variable
 601 representing the matrix formed from reading updates from σ , which could be received in any order.
 602 Upon reading all updates in σ , $\hat{A} = A$. In each such update, $\hat{A}_{i,j}$ receives the modification $w \pm 1$.
 603 As A is the adjacency matrix of an unweighted SBM, we assert without a loss of generality that
 604 an update (i, j, w) implies (j, i, w) . Furthermore, we state that positive updates $(i, j, 1)$ are only
 605 received when $\hat{A}_{i,j} = 0$ and negative updates $(i, j, -1)$ are only received when $\hat{A}_{i,j} = 1$. This is
 606 tantamount to asserting that σ represents a stream of edge additions and deletions, which can only
 607 occur if the given edge does not/does exist, respectively. Although the method remains valid without
 608 this last assumption, without it \hat{A} could at some point represent a non-simple graph.
 609

610 Given these assumptions, Subroutine D updates each of the temporary sketch variables $\hat{A}^{(1)} \equiv$
 611 $\hat{A}S_1$ and $\hat{A}^{(i)} \equiv S_{i-1}^\top \hat{A}S_i^\top$ as it receives updates from σ . We represent each of these updates
 612 (i, j, w) as the rank one matrix $U \leftarrow w\mathbf{e}_i\mathbf{e}_j^\top$, where \mathbf{e}_i and \mathbf{e}_j refer to the usual basis vectors.
 613 Applying the appropriate sketch transforms to this matrix provides us with additive updates to
 614 $\hat{A}^{(1)}, \dots, \hat{A}^{(r-1)}$. After receiving all updates, we incorporate the constant shift $q\mathbf{1}\mathbf{1}^\top$ and return
 615 the product $BS_1^\top \prod_{i=1}^{r-1} S_i BS_{i+1}^\top$.
 616

617 **Subroutine D STREAMING UPDATES TO POWER ITERATION**
618

619 1: **Input:** Integral $r > 1$, $m = O(\text{sr}(B)\varepsilon^{-2})$, stream σ of updates to A
 620 2: Sample $S_1, \dots, S_{r-1} \in \mathbb{R}^{m \times n}$
 621 3: $\hat{A}^{(1)} \leftarrow 0^{n \times m}$
 622 4: **for** $i \in \{2, \dots, r-1\}$ **do**
 623 5: $\hat{A}^{(i)} \leftarrow 0^{m \times m}$
 624 6: **end for**
 625 7: **for** update $(i, j, w) \in \sigma$ **do**
 626 8: $U \leftarrow w\mathbf{e}_i\mathbf{e}_j^\top$
 627 9: $\hat{A}^{(1)} \leftarrow US_1^\top$
 628 10: **for** $i \in \{2, \dots, r-1\}$ **do**
 629 11: $\hat{A}^{(i)} \leftarrow S_{i-1}^\top US_i^\top$
 630 12: **end for**
 631 13: **end for**
 632 14: $Q \leftarrow -q\mathbf{1}\mathbf{1}^\top$
 633 15: $BS_1^\top \leftarrow \hat{A}^{(1)} + QS_1^\top$
 634 16: **for** $i \in \{1, \dots, r-2\}$ **do**
 635 17: $S_i BS_{i+1}^\top \leftarrow \hat{A}^{(i)} + S_i QS_{i+1}^\top$
 636 18: **end for**
 637 19: $\tilde{B}^{(r)} \leftarrow BS_1^\top \prod_{i=1}^{r-1} S_i BS_{i+1}^\top$
 638 20: **Output** $\tilde{B}^{(r)}$

640 **C DEFERRED PROOFS**
641

642 Herein we present the proofs of major results excluded from the main body due to space constraints.
 643

644 **Lemma 3.1 Norms of L and row separation.** We have $\|L\|_{\text{op}} = (p - q)s_*$ and $\|L\|_{\text{F}}^2 = (p -$
 645 $q)^2 \sum_{\ell=1}^K s_\ell^2$. Moreover, rows of L^r are constant within each cluster and, if $i \in C_\ell$ and $j \in C_{\ell'}$ with
 646 $\ell \neq \ell'$,

$$\|L_{i,\cdot}^r - L_{j,\cdot}^r\|_2 = (p - q)^r \sqrt{s_\ell^{2r-1} + s_{\ell'}^{2r-1}}. \quad (19)$$

648 *Proof.* We know by definition that:
649

$$650 \quad 651 \quad L_{ij} = \begin{cases} (p - q) & \text{if } i \sim j \\ 0 & \text{if } i \not\sim j \end{cases}$$

652 It follows that L is a block diagonal matrix. We can represent it as follows:
653

$$654 \quad 655 \quad L = \begin{bmatrix} (p - q)\mathbf{1}_{s_1 \times s_1} & \mathbf{0} & \cdots & \mathbf{0} \\ \mathbf{0} & (p - q)\mathbf{1}_{s_2 \times s_2} & \ddots & \vdots \\ \vdots & \ddots & \ddots & \mathbf{0} \\ \mathbf{0} & \cdots & \mathbf{0} & (p - q)\mathbf{1}_{s_K \times s_K} \end{bmatrix} = \begin{bmatrix} u_1 v_1^T & 0 & \cdots & 0 \\ 0 & u_1 v_1^T & \ddots & \vdots \\ \vdots & \ddots & \ddots & 0 \\ 0 & \cdots & 0 & u_K v_K^T \end{bmatrix}$$

659 where

$$660 \quad 661 \quad u_j = \begin{bmatrix} 1 \\ \vdots \\ 1 \end{bmatrix}, \quad v_j = \begin{bmatrix} (p - q) \\ \vdots \\ (p - q) \end{bmatrix} \in \mathbb{R}^{s_j}.$$

664 The operator norm is then the largest of the singular values of the block matrices. Since each block
665 matrix in L is rank 1 then the operator norm bound follows by noting that

$$666 \quad 667 \quad \|u_j v_j^T\|_{op} = \|u_j\|_2 \|v_j\|_2 = \sqrt{s_j}(p - q)\sqrt{s_j} = (p - q)s_j$$

668 Furthermore, from the structure of L we can deduce that

$$669 \quad 670 \quad \|L\|_F^2 = \sum_{(i,j)} L_{ij}^2 = \sum_{\ell=1}^K (p - q)^2 s_\ell^2$$

672 The second part of the result follows from a simple counting argument after explicitly writing the
673 entries of L_{ij}^r □
674

675 **Corollary 4.3 Power chains.** If $A_1 = \cdots = A_k = B$, then with the same probability as Theorem 4.2,

$$678 \quad 679 \quad \|B S_1^\top S_1 B S_2^\top S_2 \cdots B S_{k-1}^\top S_{k-1} B - B^k\| \leq ((1 + \varepsilon)^{k-1} - 1) \|B\|^k. \quad (20)$$

680 *Proof.* Let $\widetilde{M}_1 := B$, $\widetilde{M}_{t+1} := \widetilde{M}_t S_t^\top S_t B$, and $M_t := B^t$. With $E_t := \|\widetilde{M}_t - M_t\|$ and $E_1 = 0$,

$$682 \quad 683 \quad \widetilde{M}_{t+1} - M_{t+1} = (\widetilde{M}_t - M_t) S_t^\top S_t B + \underbrace{M_t S_t^\top S_t B - M_t B}_{\text{one-step error}}.$$

685 Condition on (\widetilde{M}_t, M_t) (independent of S_t) and apply equation 4.1 twice. By a standard union
686 bound we have that with prob. $\geq 1 - 2\delta$,

$$687 \quad 688 \quad E_{t+1} \leq \varepsilon \|B\| E_t + \varepsilon \|B\|^{t+1}.$$

689 After recursively expanding the above relation satisfied by the E_t combined with the submultiplicativity of the norm we have:

$$690 \quad 691 \quad E_k \leq ((1 + \varepsilon)^{k-1} - 1) \|B\|^k.$$

692 The probability bound follows in a similar fashion as in Theorem 4.2 □

693 **Lemma 5.1 High-probability upper bound on $\text{sr}(B)$.** Let $G \sim \text{SBM}(n, K, \{s_\ell\}, p, q)$ with
694 adjacency matrix A . Let B , L , and R be defined as in equation 1. Write $s_* = \max_\ell s_\ell$ and define

$$695 \quad \sigma^2 = \max\{p(1 - p), q(1 - q)\}.$$

696 There exist constants $C_1, C_2 > 0$ such that, with probability at least $1 - 3n^{-3}$,

$$697 \quad 698 \quad 699 \quad \text{sr}(B) = \frac{\|B\|_F^2}{\|B\|_{op}^2} \leq \frac{(p - q)^2 \sum_{\ell=1}^K s_\ell^2 + n^2 \sigma^2 + C_1 n \sqrt{\log n}}{((p - q)s_* - C_2 \sigma \sqrt{n})^2}. \quad (21)$$

700 701 In particular, under the signal-dominated regime $(p - q)s_* \gg \sigma \sqrt{n}$:

702 • **Balanced case** ($s_\ell = n/K$):

704
$$\text{sr}(B) = O\left(K + \frac{K^2\sigma^2}{(p-q)^2}\right).$$

706 If additionally $(p-q)^2 \gtrsim K\sigma^2$, then $\text{sr}(B) = \Theta(K)$. More generally, under the weaker
 707 detectability condition $(p-q)^2 \gtrsim K^2\sigma^2/n$ (which follows from $(p-q)s_* \gg \sigma\sqrt{n}$ with
 708 $s_* = n/K$), we have $\text{sr}(B) = o(n)$, confirming sublinearity.

709 • **Highly imbalanced case** ($\sum_\ell s_\ell^2 \asymp s_*^2$):

711
$$\text{sr}(B) = O\left(1 + \frac{n^2\sigma^2}{(p-q)^2s_*^2}\right).$$

713 If $(p-q)s_* \gg \sigma n$, then $\text{sr}(B) = \Theta(1)$.

715 *Proof.* We first lower bound $\|B\|_{\text{op}}$ and then upper bound $\|B\|_F^2$.

717 **Lower bound on $\|B\|_{\text{op}}$:** By Weyl's inequality,

718
$$\lambda_1(B) \geq \lambda_1(L) - \|R\|_{\text{op}}.$$

720 For the expectation L of the centered matrix B , one has $\lambda_1(L) = \|L\|_{\text{op}} = (p-q)s_*$. Moreover,
 721 for the noise part R ,

722
$$\|R\|_{\text{op}} \leq C_2 \sigma \sqrt{n}$$

723 with probability at least $1 - n^{-3}$ (Lemma 2.1 of Mukherjee & Zhang (2024)). Thus, with the same
 724 probability, we have

725
$$\|B\|_{\text{op}} = \lambda_1(B) \geq (p-q)s_* - C_2 \sigma \sqrt{n}.$$

726 **Upper bound on $\|B\|_F^2$:** We start with the expansion that takes into account the symmetry of both
 727 L and R :

728
$$\|B\|_F^2 = \|L\|_F^2 + \|R\|_F^2 + 2\langle L, R \rangle.$$

730 From the definition of L it follows that:

731
$$\|L\|_F^2 = (p-q)^2 \sum_{\ell=1}^K s_\ell^2.$$

734 For R , whose entries are independent, mean zero, bounded, with $\text{Var}(R_{ij}) \leq \sigma^2$, we have

736
$$\mathbb{E}\|R\|_F^2 = \sum_{i,j} \mathbb{E}[R_{ij}^2] = \sum_{i,j} \text{Var}(R_{ij}) \leq n^2\sigma^2.$$

738 A Bernstein inequality for sums of independent bounded variables yields, with probability at least
 739 $1 - n^{-4}$,

740
$$\|R\|_F^2 \leq n^2\sigma^2 + C n \sqrt{\log n}.$$

741 Likewise, since $\langle L, R \rangle = \sum_{i,j} L_{ij} R_{ij}$ is a mean-zero sum of independent bounded variables sup-
 742 ported on the block structure of L , Bernstein implies that, with probability at least $1 - n^{-4}$,

744
$$|\langle L, R \rangle| \leq C n \sqrt{\log n}.$$

745 Combining the bounds on the terms involved in the expansion yields:

747
$$\|B\|_F^2 \leq (p-q)^2 \sum_{\ell=1}^K s_\ell^2 + n^2\sigma^2 + C_1 n \sqrt{\log n}.$$

750 Combining the above estimates using a union bound gives the final upper bound on $\text{sr}(B)$ with
 751 failure probability at most $3n^{-3}$.

752 **Balanced case analysis:** If $s_\ell = n/K$ for all ℓ , then $\sum_{\ell=1}^K s_\ell^2 = K(n/K)^2 = n^2/K$ and $s_* =$
 753 n/K . The numerator becomes:

755
$$(p-q)^2 \frac{n^2}{K} + n^2\sigma^2 + O(n\sqrt{\log n}) = n^2 \left(\frac{(p-q)^2}{K} + \sigma^2 \right) + O(n\sqrt{\log n}).$$

756 In the signal-dominated regime $(p - q)s_* \gg \sigma\sqrt{n}$, i.e., $(p - q)n/K \gg \sigma\sqrt{n}$, the denominator is:
757

$$758 \quad 759 \quad ((p - q)s_* - C_2\sigma\sqrt{n})^2 \asymp (p - q)^2 \frac{n^2}{K^2}.$$

760 Therefore:

$$761 \quad 762 \quad 763 \quad \text{sr}(B) \lesssim \frac{n^2 \left(\frac{(p-q)^2}{K} + \sigma^2 \right)}{(p-q)^2 \frac{n^2}{K^2}} = K + \frac{K^2\sigma^2}{(p-q)^2}.$$

764 For $\text{sr}(B) = \Theta(K)$, we require the second term to be $O(K)$, which holds when $(p - q)^2 \gtrsim K\sigma^2$.
765 More generally, under the weaker condition $(p - q)^2 \gtrsim K^2\sigma^2/n$, we obtain $\text{sr}(B) = O(K^2\sigma^2/(p - q)^2) = O(n)$. Since $(p - q)s_* \gg \sigma\sqrt{n}$ with $s_* = n/K$ gives $(p - q)^2n/K^2 \gg \sigma^2$, i.e., $(p - q)^2 \gg K^2\sigma^2/n$, we have $\text{sr}(B) = o(n)$, confirming sublinearity.
766
767

768 **Highly imbalanced case:** When $\sum_\ell s_\ell^2 \asymp s_*^2$, the numerator is dominated by $(p - q)^2s_*^2 + n^2\sigma^2$,
769 and the denominator (in the signal-dominated regime) is $(p - q)^2s_*^2$. Thus:
770

$$771 \quad 772 \quad \text{sr}(B) \lesssim \frac{(p - q)^2s_*^2 + n^2\sigma^2}{(p - q)^2s_*^2} = 1 + \frac{n^2\sigma^2}{(p - q)^2s_*^2}.$$

773 If $(p - q)s_* \gg \sigma n$, then the second term is $o(1)$, giving $\text{sr}(B) = \Theta(1)$. \square
774

775 **Theorem 5.3 Separation scale preservation for Algorithm B; explicit m .** Assume Assumption
776 3.2 holds for $X^* = B^r$ with parameters (a, b, Δ_r) and failure probability η . Fix $\varepsilon \in (0, 1/4)$
777 and $\delta \in (0, 1)$. Suppose S_1, \dots, S_{r-1} are independent Rademacher with
778

$$779 \quad 780 \quad m \geq C \frac{\text{sr}(B) + \log((r-1)/\delta)}{\varepsilon^2}. \quad (22)$$

781 Then, with probability at least $1 - \eta - 2\delta$, simultaneously for all $i \neq j$,
782

$$783 \quad \left| \|\tilde{B}_{i,\cdot}^{(r)} - \tilde{B}_{j,\cdot}^{(r)}\|_2 - \|B_{i,\cdot}^r - B_{j,\cdot}^r\|_2 \right| \leq \sqrt{2} \left((1 + 2\varepsilon)^{r-1} - 1 \right) \|B\|_{op}^r. \quad (23)$$

784 If, in addition, there exist some $0 < a < b$ such that
785

$$786 \quad 787 \quad \sqrt{2} \left((1 + 2\varepsilon)^{r-1} - 1 \right) \|B\|_{op}^r \leq \frac{b-a}{4} \Delta_r, \quad (24)$$

788 then the same threshold Δ_r separates within/across-cluster pairs for $\tilde{B}^{(r)}$, and single-linkage at cut
789 Δ_r recovers the largest cluster.
790

791 *Proof.* First observe that for any integer t :

$$793 \quad 794 \quad 795 \quad \text{sr}(B^t) = \frac{\|B^t\|_F^2}{\|B^t\|_{op}^2} \leq \frac{\left(\|B^{t-1}\|_{op} \|B\|_F \right)^2}{\|B\|_{op}^{2t}} \leq \text{sr}(B).$$

797 Now choosing m according to equation 14 in Theorem 5.2, forces each S_t to satisfy equation 11 with
798 accuracy 2ε and failure $\delta/(r-1)$. Corollary 4.3 then gives $\|\tilde{B}^{(r)} - B^r\| \leq ((1 + 2\varepsilon)^{r-1} - 1) \|B\|^r$
799 with prob. $\geq 1 - 2\delta$. Apply Lemma 5.2 to obtain equation 23. Assuming there are some $0 < a < b$
800 satisfying equation 24, then every within-cluster distance remains $\leq \Delta_r$ and every across-cluster
801 distance remains $\geq \Delta_r$. Union-bound the two events. \square

802 **Theorem 5.4** Let $X^* = B^r \in \mathbb{R}^{n \times n}$ with rows x_i^* . Assuming the row gap assumption 3.2 holds
803 for X^* with parameters (a, b, Δ_r) and success probability $1 - \eta$, that is: with probability $\geq 1 - \eta$,
804

$$805 \quad \|x_i^* - x_j^*\|_2 \leq a \Delta_r \quad (\text{within}), \quad \|x_i^* - x_j^*\|_2 \geq b \Delta_r \quad (\text{across}),$$

806 for some $0 < a < 1 < b$. Let $S \in \mathbb{R}^{m \times n}$ have i.i.d. mean-zero, variance- $1/m$ subgaussian entries
807 with subgaussian norm at most κ (a fixed constant). Fix $\varepsilon \in (0, 1)$ and $\delta \in (0, 1)$. If
808

$$809 \quad m \geq \frac{C(\kappa)}{\varepsilon^2} \left(\log n + \log \frac{1}{\delta} \right), \quad (25)$$

810 then with probability at least $1 - \eta - \delta$ the following holds simultaneously for all $i \neq j$:

$$812 \quad (1 - \varepsilon) \|x_i^* - x_j^*\|_2 \leq \|S(x_i^* - x_j^*)\|_2 \leq (1 + \varepsilon) \|x_i^* - x_j^*\|_2.$$

813 Consequently, if

$$814 \quad (1 + \varepsilon) a < (1 - \varepsilon) b, \quad (26)$$

815 There exists a threshold $\tilde{\Delta} \in ((1 + \varepsilon)a\Delta_r, (1 - \varepsilon)b\Delta_r)$ that separates within- and across-cluster
816 pairs for the sketched rows $\{Sx_i^*\}$; hence, the thresholding step in Algorithm 1 recovers the largest
817 cluster.
818

819 *Proof. Step 1: JL preservation for a fixed finite set.* Let \mathcal{J} be the event that S preserves all
820 pairwise distances among $\{x_i^*\}_{i=1}^n$ within a factor $1 \pm \varepsilon$. For subgaussian maps with parameter
821 κ , the Johnson-Lindenstrauss lemma (via Hanson-Wright or standard subgaussian concentration)
822 ensures that equation 25 implies

$$824 \quad \mathbb{P}(\mathcal{J}) \geq 1 - \delta, \quad \text{and on } \mathcal{J} : \quad (1 - \varepsilon)\|u\| \leq \|Su\| \leq (1 + \varepsilon)\|u\| \quad \forall u \in \{x_i^* - x_j^*\}.$$

826 **Step 2: Intersect with Assumption 3.2** Let \mathcal{A} be the Assumption 3.2 event (success $\geq 1 - \eta$). A
827 union bound yields

$$828 \quad \mathbb{P}(\mathcal{A} \cap \mathcal{J}) \geq 1 - \eta - \delta.$$

829 We henceforth work on $\mathcal{A} \cap \mathcal{J}$.

830 **Step 3: Threshold separation after sketching.** For any within-cluster pair, \mathcal{A} gives $\|x_i^* - x_j^*\|_2 \leq$
831 $a\Delta_r$, and then \mathcal{J} implies

$$833 \quad \|S(x_i^* - x_j^*)\|_2 \leq (1 + \varepsilon)a\Delta_r.$$

834 For any across-cluster pair, \mathcal{A} gives $\|x_i^* - x_j^*\|_2 \geq b\Delta_r$, and then \mathcal{J} implies

$$835 \quad \|S(x_i^* - x_j^*)\|_2 \geq (1 - \varepsilon)b\Delta_r.$$

837 If the margin condition equation 26 holds, these ranges are disjoint, so any $\tilde{\Delta} \in ((1 + \varepsilon)a\Delta_r, (1 -$
838 $\varepsilon)b\Delta_r)$ separates the two classes, and the thresholding step in Algorithm 1 succeeds. The theorem
839 follows by taking $\tilde{\Delta} = \Delta_r$ when $(1 + \varepsilon)a \leq 1 \leq (1 - \varepsilon)b$. \square
840

841
842
843
844
845
846
847
848
849
850
851
852
853
854
855
856
857
858
859
860
861
862
863